Cell

Identification of Positionally Distinct Astrocyte Subtypes whose Identities Are Specified by a Homeodomain Code

Christian Hochstim,[1] Benjamin Deneen,[1] Agnès Lukaszewicz,[1] Qiao Zhou,[2] and David J. Anderson[1,*]
[1]Division of Biology 216-76, Howard Hughes Medical Institute, California Institute of Technology, Pasadena, CA 91125, USA
[2]Present address: The Biological Laboratories, Harvard University, 16 Divinity Avenue, Cambridge, MA 02138, USA.
*Correspondence: wuwei@caltech.edu
DOI 10.1016/j.cell.2008.02.046

SUMMARY

Astrocytes constitute the most abundant cell type in the central nervous system (CNS) and play diverse functional roles, but the ontogenetic origins of this phenotypic diversity are poorly understood. We have investigated whether positional identity, a fundamental organizing principle governing the generation of neuronal subtype diversity, is also relevant to astrocyte diversification. We identified three positionally distinct subtypes of white-matter astrocytes (WMA) in the spinal cord, which can be distinguished by the combinatorial expression of Reelin and Slit1. These astrocyte subtypes derive from progenitor domains expressing the homeodomain transcription factors Pax6 and Nkx6.1, respectively. Loss- and gain-of-function experiments indicate that the positional identity of these astrocyte subtypes is controlled by Pax6 and Nkx6.1 in a combinatorial manner. Thus, positional identity is an organizing principle underlying astrocyte, as well as neuronal, subtype diversification and is controlled by a homeodomain transcriptional code whose elements are reutilized following the specification of neuronal identity earlier in development.

INTRODUCTION

A central problem in neural development is to elucidate the mechanisms that control the ontogenetic diversification of neuronal and glial subtypes in the central nervous system (CNS). In the last decade, positional identity has emerged as one of the fundamental organizing principles governing neuronal subtype diversification. In the ventral spinal cord, for example, molecularly distinct subtypes of motoneurons (MNs) and interneurons (INs) are generated from spatially segregated domains of progenitor cells, arranged along the dorsoventral axis of the ventricular zone (VZ) (Burrill et al., 1997; Ericson et al., 1997; Briscoe et al., 1999). These progenitor domains are generated by a combinatorial code of homeodomain (HD) transcription factors, whose expression patterns are initially established by graded morphogen signaling, and further refined by cross-repressive interactions (Briscoe et al., 2000; Goulding and Lamar, 2000; Jessell, 2000; McMahon, 2000).

While astrocytes are the most abundant cell type in the CNS, play varied functional roles (reviewed in Fields and Stevens-Graham, 2002; Ullian et al., 2004) and exhibit phenotypic heterogeneity (see below), there has been relatively little consideration of positional identity as an organizing feature of astrocyte diversity or of positional specification as a mechanism underlying astrocyte diversification. The existence of different subtypes of astrocytes, such as fibrous and protoplasmic, has long been recognized based on morphologic (Vaughn and Pease, 1967; Mori and Leblond, 1969) and antigenic (Raff et al., 1984; Raff, 1989) criteria. However, these subtypes are thought to spatially segregate primarily according to their location in either gray or white matter (Miller and Raff, 1984). It has been speculated that spinal cord astrocytes may exhibit regional distinctions, based on studies of astrocyte phenotypes in vitro (reviewed in Miller et al., 1994), but whether such phenotypes are positionally distinct in vivo or established by positional specification mechanisms was not established. Morphologically distinct astrocyte subtypes have been identified in different layers of the olfactory bulb (Bailey and Shipley, 1993), and astrocytes with different electrophysiological properties have been described in hippocampal areas CA1 and CA3 (D'Ambrosio et al., 1998). However, with few molecular markers to differentiate these subtypes in vivo (Sharif et al., 2004), it has been difficult to study their ontogeny, phenotypic stability, and function.

There is some evidence for positional heterogeneity among astrocyte precursors in the spinal cord. The bHLH transcription factor SCL is specifically expressed in the p2 progenitor domain (Briscoe et al., 2000) and is required for generic aspects of astrocyte differentiation within this domain (Muroyama et al., 2005). However, these data did not provide evidence that differentiated p2-derived astrocytes are phenotypically distinct from those derived from other progenitor domains. Expression of FGFR3 is initially restricted to p2-derived astrocyte precursors (Pringle et al., 2003) but later expands to astrocytes at other positions along the dorsoventral axis (Deneen et al., 2006). The expression of several patterning molecules controlling neuronal identity is maintained in the VZ, during the transition from the neurogenic to the gliogenic phase of development (Fu et al., 2003; Ogawa et al.,

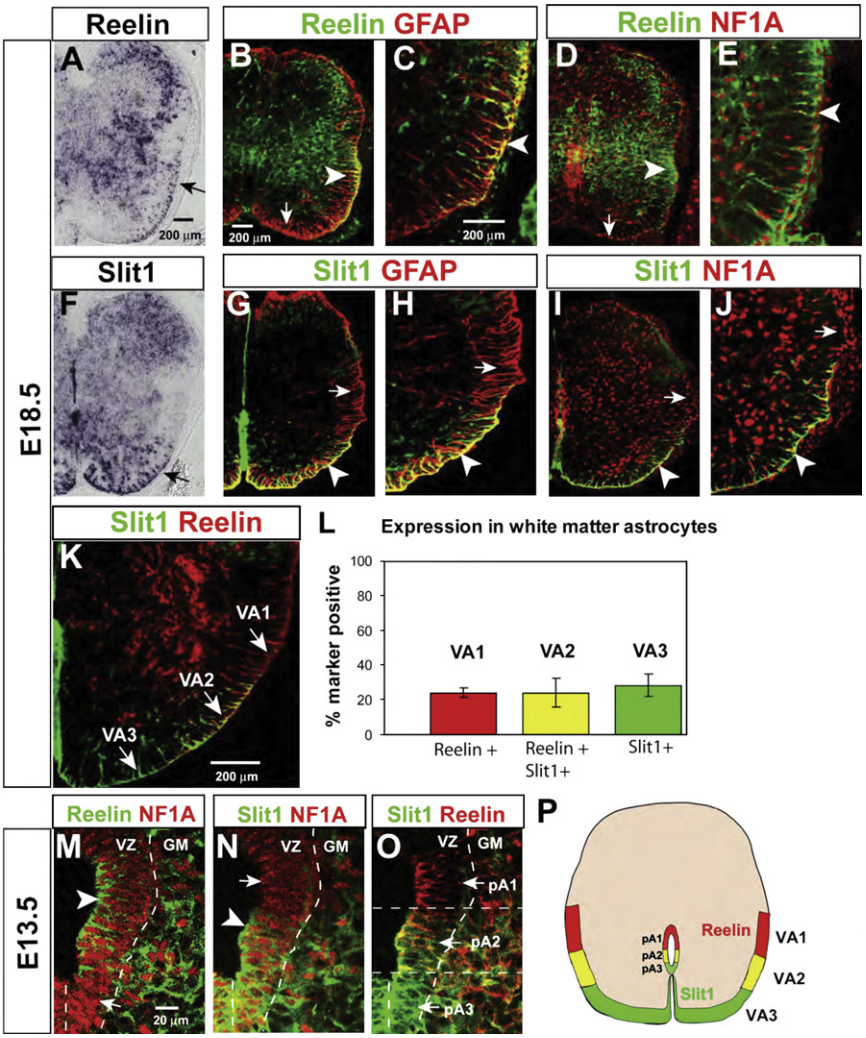

Figure 1. Reelin and Slit1 Define Astrocyte Subpopulations in the Ventral Spinal Cord

(A–F) In situ hybridization for mouse Reelin and Slit1 mRNAs (A and F). Arrows indicate expression in ventral white matter. Double-label immunohistochemistry for Reelin and GFAP (B–C) or NFIA (D–E) are shown. Arrowheads indicate double-positive cells in lateral white matter; arrows indicate Reelin$^-$ astrocytes in ventral white matter.

(G–J) Double-label immunohistochemistry for *Slit1*-GFP and either GFAP (G and H) or NFIA (I and J), in *Slit1*$^{GFP/+}$ embryos. Arrowheads indicate Slit1$^+$ astrocytes in ventral white matter, arrows Slit1$^-$ astrocytes in the lateral white matter.

(K) Double labeling for Reelin and Slit1-GFP reveals three subpopulations of ventral astrocytes (arrows).

(L) Quantification of the percentage of NFIA$^+$ astrocytes expressing each of the three markers. Data represent the mean ± SEM of six or six sections per embryo from three embryos.

(M–O) Triple labeling for Reelin, Slit1-GFP, and NFIA in the E13.5 ventral VZ, displayed as pairwise comparisons from the same section. Arrowheads and arrows in (M) and (N) indicate NFIA$^+$ cells that are positive or negative, respectively, for Reelin (M) or Slit1 (N). In (O), overlay of Slit1 and Reelin reveals three adjacent progenitor domains in the VZ.

(P) Composite schematic illustrating positions of VA1–VA3 astrocytes in the white matter at E18.5 and corresponding progenitor domains (pA1-3) in the VZ at E13.5.

2005; Deneen et al., 2006; Sugimori et al., 2007), and it has been speculated that this may indicate the existence of positionally distinct astrocyte subtypes (Ogawa et al., 2005). However, no evidence has been presented for the existence of such subtypes in the white matter.

Here we identify three positional distinct subpopulations of white-matter astrocytes (WMAs) in the ventral spinal cord, and characterize a homeodomain code that is required for their specification in the ventricular zone. Our data indicate that positional identity is an organizing feature of astrocyte, as well as neuronal, diversity in the CNS and is controlled by similar molecular mechanisms.

RESULTS

Reelin and Slit1 Mark Subpopulations of WMAs in Ventral Spinal Cord

We initially identified Reelin and Slit1 as astrocyte markers in a gene expression-profiling screen for targets of Olig2. In *Olig2* mutants, Olig2$^+$ progenitors generate astrocytes instead of oligodendrocytes, at gliogenic stages (Lu et al., 2002; Zhou and Anderson, 2002). Expression profiling of Olig2-GFP-expressing glial progenitors isolated from *Olig2* mutant versus wild-type spinal cord (Gabay et al., 2003; Mukouyama et al., 2006) (see Experimental Procedures) identified Reelin and Slit1 mRNAs as upregulated in *Olig2*$^{-/-}$ cells, suggesting that they might be expressed by astrocyte progenitors. In situ hybridization to embryonic day 18.5 (E18.5) spinal cord sections indicated that Reelin and Slit1 mRNAs are expressed by a subset of cells at the margins of the white matter (Figures 1A and 1F, arrows).

To confirm that Reelin and Slit1 are expressed by WMAs, we performed double-labeling studies using the generic astrocyte markers GFAP, a glial-specific intermediate filament, or NFIA, a nuclear protein expressed in differentiated astrocytes and their precursors (Deneen et al., 2006), together with antibodies to Reelin or to GFP in a *Slit1-GFP* reporter mouse (Plump et al., 2002). In the white matter of E18.5 spinal cord, both Reelin and Slit1 were expressed by astrocytes (Figures 1B–1E and 1G–1J, arrowheads), but not by Olig2$^+$ oligodendrocytes (data not shown). Both Reelin and Slit1 were also expressed by neurons in the gray matter, as previously reported (Holmes et al., 1998; Brose et al., 1999; Kubasak et al., 2004; Yip et al., 2004a). The morphology of both Reelin$^+$ and Slit1$^+$ white-matter cells is characteristic of WMAs (Liuzzi and Miller, 1987), with NFIA$^+$ nuclei localized at the subpial surface (Figures 1E and 1J, arrowheads)

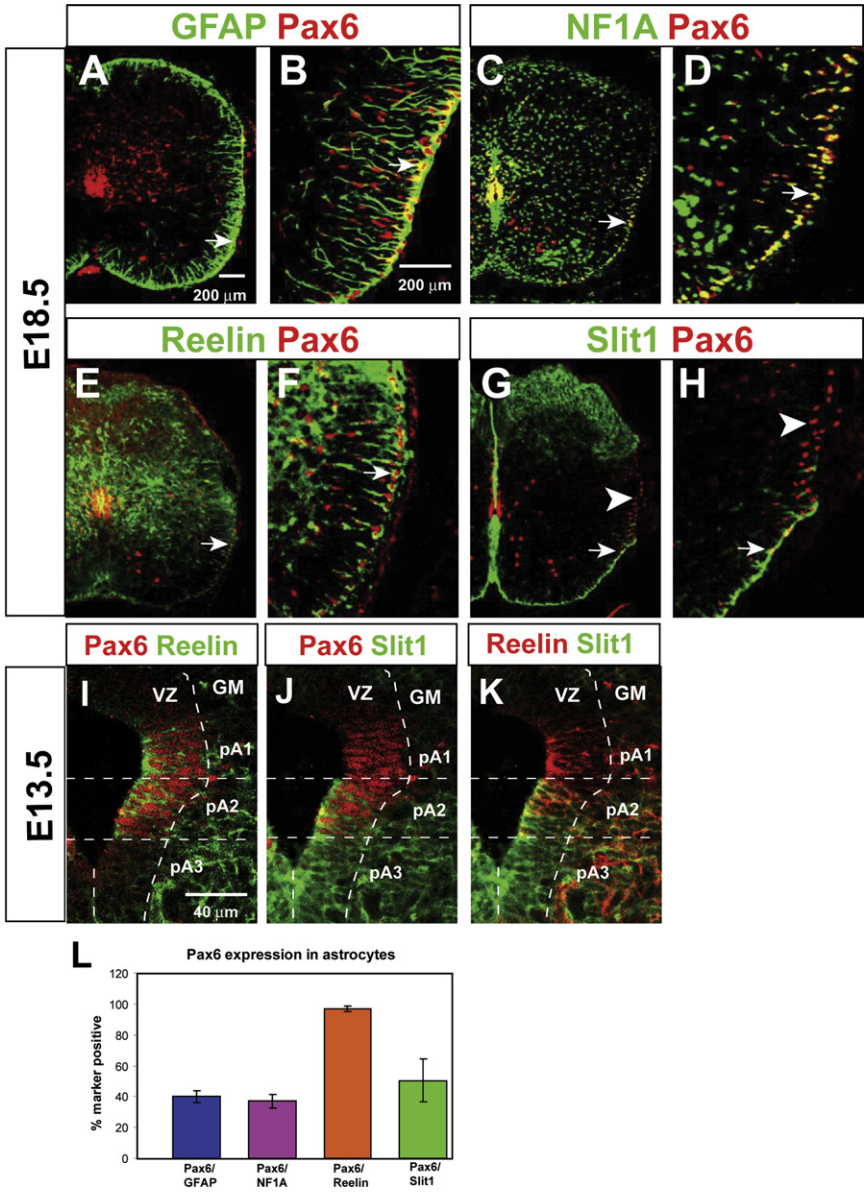

Figure 2. Expression of Pax6 in Reelin$^+$ Astrocytes and Their Precursors

(A–H) Double labeling for Pax6 (red) and the indicated markers (green) at E18.5. (B), (D), (F), and (H) are higher magnification views of the areas indicated by arrows in (A) (C), (E), and (G), respectively.

(I–K) Triple labeling for Pax6, Reelin, and Slit1-GFP in the E13.5 ventral VZ, displayed as pairwise comparisons from the same section.

(L) Quantification of Pax6 expression among total (GFAP$^+$ or NFIA$^+$) astrocytes, and Reelin$^+$ or Slit1$^+$ WMAs. Error bars represent mean ± SEM.

and radially oriented GFAP$^+$ processes projecting inward (Figures 1C and 1H, arrowheads; see also Figure S1).

Unexpectedly, we found that Reelin and Slit1 were not expressed by all astrocytes, but rather by positionally distinct subsets in the ventral white matter. Reelin was expressed in the dorsolateral and ventrolateral white matter, but not in astrocytes close to the ventral midline (Figures 1A and 1B; arrow and arrowhead, respectively). Slit1, conversely, was expressed in astrocytes in the ventromedial and ventrolateral white matter, but not in the dorsolateral white matter (Figures 1F and 1G; arrow and arrowhead, respectively). Double labeling for Reelin and Slit1 revealed the existence of three adjacent domains of WMAs: a dorso-lateral domain of Reelin$^+$, Slit1$^-$ cells; a ventro-lateral domain of Reelin$^+$, Slit1$^+$ cells; and a ventro-medial domain of Slit1$^+$, Reelin$^-$ cells (Figure 1K). For convenience, we refer to these subpopulations henceforth as ventral astrocyte subtypes 1, 2, and 3 (VA1, VA2, and VA3, respectively; Figures 1K and 1P). Quantification indicated that each of these three subpopulations is present in roughly equal numbers (Figure 1L).

In principle, VA1–VA3 phenotypes could be established after astrocyte precursors migrate to the WM, under the influence of local environmental cues, or could be specified by positional mechanisms prior to emigration from the VZ. As a first step toward addressing this question, we asked whether Reelin and Slit1 were expressed by positionally distinct subsets of astrocyte precursors within the neuroepithelium. Examination of spinal cord sections at E13.5, a stage when most astrocyte precursors have been specified in the ventral VZ (Shibata et al., 1997; Ogawa et al., 2005; Deneen et al., 2006), revealed that Reelin and Slit1 are expressed in cells within the germinal layer. Triple labeling for Reelin, Slit1-GFP, and NFIA indicated that Reelin and Slit1 are expressed by NFIA$^+$ glial precursors (Figures 1M and 1N, arrowheads) and that the domains of their expression partially overlap (Figure 1O). This partial overlap subdivides the ventral-most VZ into three domains: a dorsal-most Reelin$^+$, Slit1$^-$ domain; a more ventral Reelin$^+$, Slit1$^+$ domain; and a ventro-medial Reelin$^-$, Slit1$^+$ domain (Figure 1O). The spatial organization of these progenitor domains, which we refer to as pA1, pA2, and pA3, respectively, therefore mirrors that of the VA1, VA2, and VA3 domains in the WM (Figure 1P).

Pax6 Marks Reelin$^+$ Astrocytes

Our microarray analysis also indicated that Pax6 mRNA was upregulated, together with Reelin and Slit1, in the *Olig1,2*$^{-/-}$ population. Double-labeling experiments indicated that Pax6 marks a subpopulation of astrocytes in the ventro-lateral white matter (Figures 2A–2D), whose distribution is similar to that of Reelin$^+$ astrocytes (Figures 2E–2F). Pax6$^+$ cells constitute approximately 40% of all GFAP$^+$ and NF1A$^+$ WMAs (Figures 2A–2D and 2L).

Double labeling for Reelin and Pax6 confirmed that 100% of Reelin$^+$ astrocytes coexpress Pax6, suggesting that Pax6 marks the VA1 and VA2 subpopulations (Figures 2E, 2F [arrows], and 2L). Since Slit1$^+$ astrocytes are equally distributed between the VA3 and VA2 populations, ~50% of Slit1$^+$ astrocytes (VA2) should be Pax6$^+$, and this was indeed the case (Figure 2H [arrow versus arrowhead] and 2L). Pax6 was excluded from the ventromedial domain of Slit1 expression (Figure 2G), corresponding to the VA3 subset. In the VZ at E13.5, triple labeling for Pax6, Reelin, and Slit1 indicated that the spatial relationship between expression of the HD factor and the two astrocyte markers was similar to that observed in the white matter at E18.5: Pax6 overlapped with all of the Reelin-expressing progenitors (Figure 2I) and a subset of the Slit1-expressing progenitors (Figure 2J).

To investigate whether Pax6$^+$ cells in the VZ are precursors of Pax6$^+$ WMAs, we pulse-labeled embryos at E13.5 with BrdU, and chased to E15.5 or E18.5. We observed a progressive shift in the distribution of both total Pax6$^+$ cells, and of BrdU-labeled Pax6$^+$ cells, from the VZ to the mantle zone (MZ) to the WM, during the chase period (Figure S2J and S2K). The proportion of Pax6$^+$ cells in the WM increased ~2.5-fold from E15.5 to E18.5, and this increase could be quantitatively accounted for by assuming that, during the same interval, Pax6$^+$ cells in the VZ migrate to the MZ, and from the MZ to the WM (see Figure S2 and its corresponding legend). The most parsimonious interpretation of these data is that at least some Pax6$^+$ cells in the E13.5 VZ are precursors of Pax6$^+$ WMAs.

Pax6 Is Required for Reelin Expression in Astrocytes

Pax6 has been shown to control the positional identity of a subset of INs in the ventral spinal cord (Burrill et al., 1997; Ericson et al., 1997). We therefore asked whether it might also play a role in the determination of astrocyte positional identity. *Pax6$^{lacZ/lacZ}$* homozygous mutants (St-Onge et al., 1997) exhibited a striking reduction in Reelin mRNA expression in the ventro-lateral white matter at E18.5, while expression in the gray matter appeared only modestly reduced (Figures 3A and 3B, versus 3E and 3F; arrows versus arrowheads, respectively). Immunostaining confirmed a loss of Reelin expression in GFAP$^+$ and NFIA$^+$ astrocytes (Figures 3C and 3D versus 3G and 3H; arrows versus arrowheads). Quantification indicated a strong and statistically significant reduction in both the percentage (Figure 3I) and absolute number (Figure 3J) of Reelin$^+$ astrocytes, using either GFAP or NFIA as counterstains.

We detected no reduction in the total number of astrocytes in the spinal cord of E18.5 *Pax6* mutant embryos (Figure 3J, GFAP$^+$ and NFIA$^+$), consistent with an earlier analysis using GLAST as a generic astrocyte marker (Ogawa et al., 2005). Since Reelin$^+$ cells constitute ~60% of all ventral WMAs, this argues against the idea that Reelin$^+$ astrocytes selectively die in the absence of Pax6; otherwise there should be a measureable reduction in overall astrocyte number. However, it is possible that the mutation could cause the selective death of Pax6$^+$ astrocytes, which is then compensated by the expansion of other, Pax6$^-$, astrocyte subpopulations. To address this possibility, we employed the marker gene *lacZ*, present in the *Pax6* knockout allele (St-Onge et al., 1997) to trace the fate of Pax6$^+$ cells in the absence of Pax6 function. The percentage of Pax6$^+$ or β-gal$^+$ cells that expressed GFAP or NFIA was identical in wild-type and mutant embryos, respectively (Figure 3I; GFAP$^+$, [Pax6$^+$ or β-gal$^+$]; NFIA$^+$ [Pax6$^+$ or β-gal$^+$]). Thus, the loss of *Pax6* did not produce a failure of generic astrocyte differentiation by Pax6$^+$ cells. Furthermore, the absolute number of GFAP$^+$, Pax6$^+$ (or GFAP$^+$-β-gal$^+$) cells was unaffected in the mutant (Figure 3J; [Pax6$^+$ or β-gal$^+$], GFAP$^+$), confirming that there was no selective death of Pax6$^+$ astrocytes. However, there was a strong reduction in the percentage of Pax6-β-gal$^+$ cells that were Reelin$^+$ in the mutant, compared to wild-type (Figure 3I, Reelin$^+$/[Pax6$^+$ or β-gal$^+$]). Taken together, these data indicate that Pax6 is required for the expression of Reelin in VA1 and VA2 astrocytes, but not for their generic differentiation to astrocytes, migration to the white matter or survival.

Dorsal Expansion of Astrocytic Slit1 Expression in the Absence of Pax6

The foregoing analysis left open the question of whether the loss of *Pax6* function simply caused a failure of Reelin expression by astrocytes, or rather a change in the positional identity of VA1 astrocytes. In the latter case, one might expect that presumptive VA1 astrocytes would acquire a Slit1$^+$ phenotype. Due to a lack of adequate antibodies to Slit1, we intercrossed the Pax6-lacZ mice with Slit1-GFP mice, and analyzed the expression of *Slit1*-GFP in *Pax6* mutants (*Slit$^{GFP/+}$*; *Pax6$^{lacZ/lacZ}$*). In *Pax6* mutant embryos, there was a significant increase in the percentage of GFAP$^+$ or NFIA$^+$ astrocytes that expressed Slit1-GFP (Figure 3Q, red bars). Moreover, the spatial domain of Slit1-GFP expression appeared to expand dorsally in the mutant (Figures 3K–3M versus 3N–3P; arrows). Most importantly, the percentage of Pax6$^+$ astrocytes that expressed Slit1 increased from approximately 50%–60% in wild-type embryos to virtually 100% in the mutant (Figure 3Q, Slit1$^+$/Pax6$^+$ or β-gal$^+$), reflecting the acquisition of Slit1 expression by dorsal Pax6-β-gal$^+$ cells (Figures 3M and 3P, arrows). Taken together, these data indicate that in the absence of Pax6 function, not only is Reelin expression lost, but Slit1 expression is derepressed, in VA1-type astrocytes (Figure 3R). This suggests that loss of Pax6 causes a ventralization of the VA1 domain, such that supernumerary VA3 astrocytes are now found in a more dorsal, ectopic location, analogous to the phenotypes of other spinal cord patterning mutations that change the number and distribution of interneuron subtypes (Jessell, 2000; Shirasaki and Pfaff, 2002).

Pax6 Is Sufficient to promote Reelin and Repress Slit1 Expression in Astrocytes

To investigate whether Pax6 plays an instructive role in regulating the expression of markers of astrocyte positional identity, we performed in vivo gain-of-function experiments in the embryonic chick neural tube. We first examined Reelin and Slit1 expression in the unmanipulated E12 chick spinal cord to confirm that these genes labeled subsets of WMAs, as in the mouse. We observed white-matter domains containing Reelin$^+$/Slit1$^-$, Reelin$^+$/Slit1$^+$ and Reelin$^-$/Slit1$^+$ VA1–VA3, astrocytes, as in the mouse (Figure S3). We therefore examined the effect of Pax6 misexpression on these ventral astrocyte populations. The spinal cord of E2 chick embryos was electroporated with replication competent

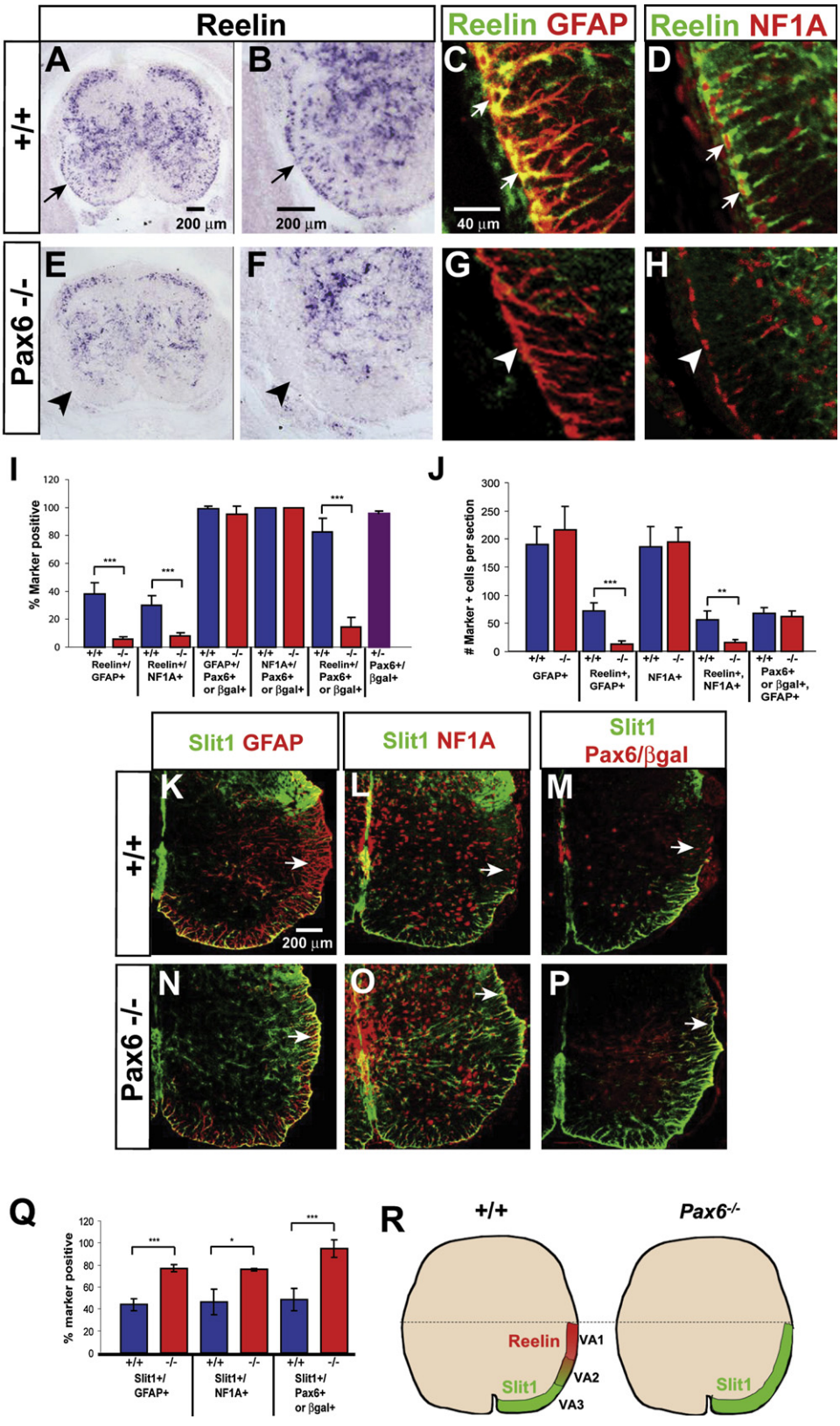
Reelin
Reelin GFAP
Reelin NF1A
+/+
Pax6 -/-
A
B
C
D
E
F
G
H
200 μm
40 μm
I
% Marker positive
Reelin+/ GFAP+
Reelin+/ NF1A+
GFAP+/ Pax6+ or βgal+
NF1A+/ Pax6+ or βgal+
Reelin+/ Pax6+ or βgal+
Pax6+/ βgal+
J
Marker + cells per section
GFAP+
Reelin+, GFAP+
NF1A+
Reelin+, NF1A+
Pax6+ or βgal+, GFAP+
Slit1 GFAP
Slit1 NF1A
Slit1 Pax6/βgal
K
L
M
N
O
P
Q
% marker positive
Slit1+/ GFAP+
Slit1+/ NF1A+
Slit1+/ Pax6+ or βgal+
R
+/+
Pax6-/-
Reelin
Slit1
VA1
VA2
VA3

RCAS(B) retroviruses carrying either the chick Pax6 or GFP genes. Electroporated embryos were harvested and analyzed at E12, following 10 days of development in ovo. Pax6 misexpression significantly increased the percentage of Reelin$^+$ cells among NFIA$^+$ cells in the white matter, compared with control GFP misexpressing embryos (Figure 4F versus 4H, WM; Figure 4CC, Reelin, E). The total number of NFIA$^+$ astrocytes was not affected by Pax6 electroporation (data not shown). These data indicate that Pax6 is sufficient, as well as necessary, for Reelin expression by ventral astrocytes in vivo.

Because we observed Pax6$^+$, Reelin$^+$ cells in the VZ as well as in the white matter (Figure 2I); we also asked whether misexpression of Pax6 could promote a ventral expansion of the domain of Reelin expression in this germinal layer. We therefore examined embryos at E5, a stage at which ventral VZ progenitors are specified for a glial fate (Shibata et al., 1997; Deneen et al., 2006). Pax6 misexpression indeed promoted a ventral expansion of Reelin expression within the VZ (Figure S4C [arrow] and S4M). Importantly, a similar result was obtained when electroporation was performed at E4.5, by which time neurogenesis has largely ceased in the ventral region of the VZ (Deneen et al., 2006) (Figure S4I [arrow] and S4M). This ventral expansion of Reelin expression occurred in NFIA$^+$ cells (Figures S4B and S4H, arrows), which are likely glial precursors (Deneen et al., 2006). The fact that this phenotype can be observed in embryos electroporated after ventral neurogenesis has terminated suggests a direct role for Pax6 to control Reelin expression in glial precursors, rather than an indirect role mediated by earlier effects on neuronal precursors. In support of this conclusion, we were able to observe changes in Reelin expression, caused misexpression of Pax6, at axial levels where there was no change in the number or distribution of ventral interneuron subtypes whose development is Pax6 dependent (Burrill et al., 1997; Ericson et al., 1997; Osumi et al., 1997) (data not shown).

The derepression of Slit1 observed in *Pax6*$^{-/-}$ embryos predicted that misexpression of *Pax6* might downregulate Slit1 expression in WMAs. Indeed, we observed a significant reduction in the percentage of Slit1$^+$; NFIA$^+$ astrocytes in the ventral region of Pax6-electroporated embryos, compared to GFP-electroporated controls (Figure 4R versus 4T, WM; Figure 4CC, Slit1). Pax6 misexpression also caused a mild, but detectable, downregulation of Slit1 mRNA in the VZ at E5 (data not shown). Thus, Pax6 is sufficient, as well as necessary, for Slit1 repression in a subset of astrocytes and their presumptive precursors. Taken together, these data suggest that Pax6 plays an instructive role in regulating astrocyte positional identity, through positive and negative regulation of Reelin and Slit1, respectively.

Expression of Nkx6.1 by Slit1$^+$ Astrocytes and Their Precursors

The observation that Pax6 promotes expression of Reelin and represses that of Slit1, explained the VA1 phenotype, but raised the question of how VA2 astrocytes can express Slit1, given that they are also Pax6$^+$. One possibility is that repression of Slit1 by Pax6 requires a cofactor, which is present in VA1 astrocytes but lacking in VA2 astrocytes. This seemed unlikely, since Pax6 was able to repress Slit1 in ventral (VA3) WMAs, in gain-of-function experiments. Alternatively, VA2 astrocytes may contain a factor absent in VA1 astrocytes, which promotes Slit1 expression and/or neutralizes the repressive activity of Pax6 toward Slit1. One candidate for the latter activity is Nkx6.1, an HD transcription factor expressed in the ventral VZ at both neurogenic and gliogenic (Fu et al., 2003) stages. Expression of Nkx6.1 partially overlaps that of Pax6 in the p2 and pMN domains while the more dorsal p0 and p1 domains express Pax6 but not Nkx6.1 (Briscoe et al., 2000; Jessell, 2000; Briscoe and Ericson, 2001). We therefore investigated the possibility that expression of Slit1 in WMAs is under the control of Nkx6.1.

We first compared the expression of Nkx6.1 and Slit1 in E18.5 spinal cord WMAs. Triple labeling for GFAP, Nkx6.1, and Slit1-GFP revealed that Nkx6.1 is expressed in WMAs (Figure 5A–5C, arrows), and that the dorso-ventral domain of its expression is approximately coextensive with that of Slit1 (Figure 5A, 5B, and 5D). Quantification indicated that >90% of Slit1$^+$ WMAs are Nkx6.1$^+$ (Figure 5J, green bar). We next asked whether Pax6 and Nkx6.1 are coexpressed in the region of the white matter where VA2 astrocytes (Pax6$^+$, Slit1$^+$) are located. Triple labeling revealed an overlap of Pax6 and Nkx6.1 expression in the ventrolateral white matter, within Slit1$^+$ cells (Figures 5E–5I, arrows). Quantification indicated that virtually 100% of Pax6$^+$, Slit1$^+$ cells were Nkx6.1$^+$ (Figures 5I and 5J, arrows and turquoise bar, respectively). These data support the idea that VA2 astrocytes are Nkx6.1$^+$, Pax6$^+$, and Slit1$^+$. (It was not possible to directly compare Nkx6.1 and Reelin expression in these experiments, due to antibody incompatibility).

In addition to their coexpression in the white matter, Nkx6.1 and Slit1 are coexpressed in the VZ, where the dorsal boundaries of their expression domains are coextensive (Figure 5K). Triple labeling for Pax6, Nkx6.1, and Slit1-GFP indicated that the domain of Pax6 expression that overlaps that of Slit1 (Figure 5M,

Figure 3. Astrocyte Subtype Conversion in *Pax6*$^{-/-}$ Mice

(A–H) Shown in (A), (B), (E), and (F) is in situ hybridization for Reelin mRNA in E18.5 spinal cord of wild-type (A and B) and *Pax6* mutant (E and F) embryos. (B) and (F) are higher-magnification views of (A) and (E), respectively. Arrows in (A) and (B) indicate Reelin$^+$ cells in the white matter.Shown in (C), (D), (G), and (H) are double labeling for Reelin and GFAP (C and G) or NFIA (D and H) in wild-type (C and D) and *Pax6* mutant (G and H) embryos.

(I and J) Quantification of Reelin expression by WMAs in E18.5 wild-type (blue bars) and *Pax6*$^{-/-}$ (red bars) spinal cord. In (I), the percentage of total GFAP$^+$ or NFIA$^+$ WMAs expressing Reelin is significantly reduced in the *Pax6*$^{lacZ/lacZ}$ mutant (***, $p < .001$). In (J), the absolute number of GFAP$^+$ and NFIA$^+$ astrocytes in the white matter is not changed in the *Pax6*$^{lacZ/lacZ}$ spinal cord, nor is the average number of Pax6$^+$ GFAP$^+$ astrocytes. (*** and **, $p < .001$ and .002, respectively). The data are derived from five wild-type and six mutant embryos from three independent litters.

(K–P) Spinal cord sections from *Pax6*$^{+/+}$; *Slit1*$^{GFP/+}$ (K–M) and *Pax6*$^{lacZ/lacZ}$; *Slit1*$^{GFP/+}$ (N–P) embryos double labeled for the indicated markers. Arrows indicate VA1 astrocytes (K–M) that exhibit derepression of Slit1 in the mutant (N–P). Red staining in (M) and (P) represents anti-Pax6 (M) or anti-β-gal (P).

(Q) Slit1 expression among total astrocytes (GFAP$^+$ or NFIA$^+$) is significantly increased in *Pax6*$^{-/-}$ embryos (*** and *, $p = .0003$, and .012, respectively). Error bars represent mean ± SEM.

(R) Schematic illustrating the changes in Reelin and Slit1 expression by ventral astrocytes in the Pax6 mutant.

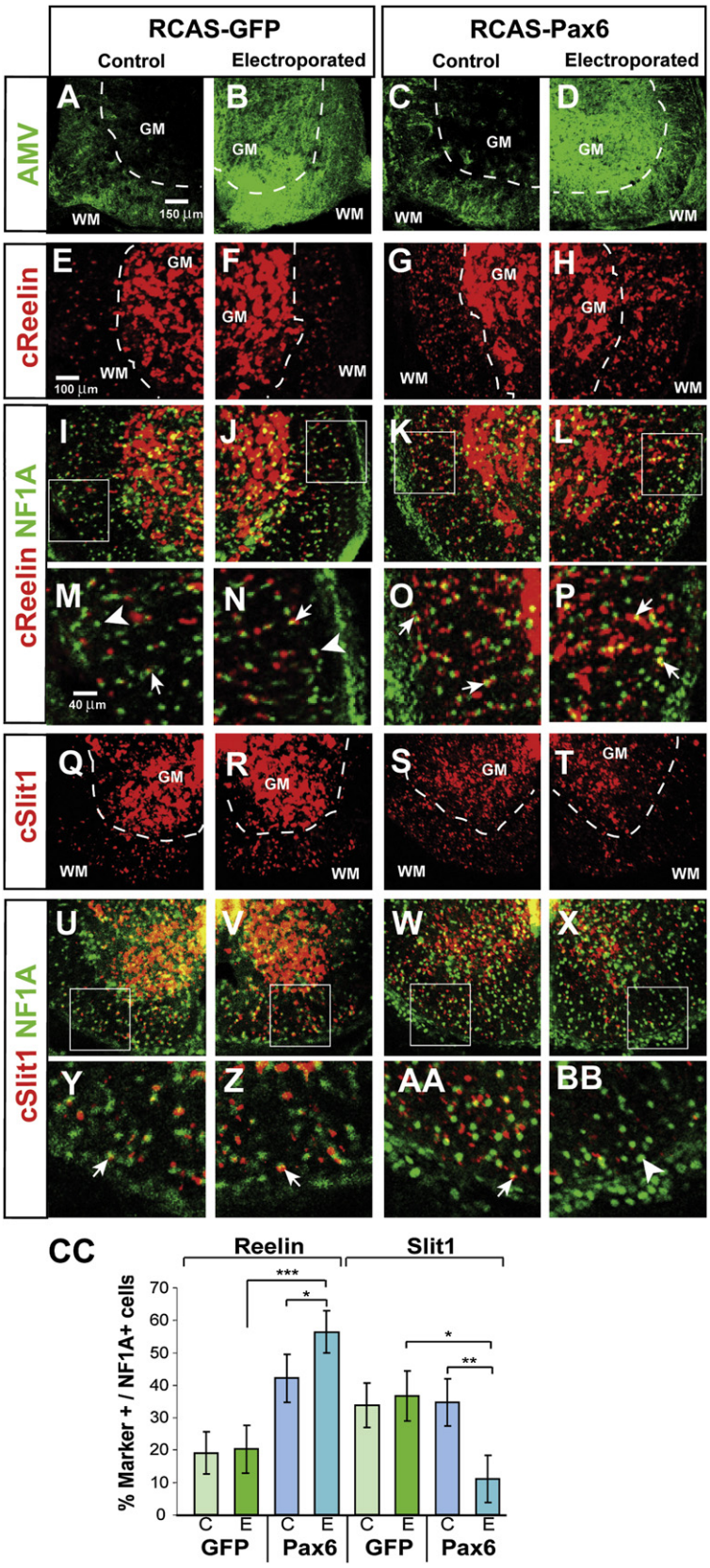

Figure 4. Pax6 Is Sufficient to Promote Reelin Expression and Repress Slit1 Expression in Astrocytes

(A–D) Immunostaining for RCAS retroviral coat protein AMV in E12 spinal cord of chick embryos electroporated with either RCAS-GFP (A and B) or RCAS-Pax6 (C and D). "WM," white matter; "GM," gray matter.

(E–BB) Antibody staining for NFIA combined with fluorescent in situ hybridization for Reelin (E–P) or Slit1 (Q–BB) mRNAs. (I)–(L) and (U)–(X) are the same panels as in (E)–(H) and (Q)–(T), respectively, but include NF1A expression. (M)–(P) and (Y)–(BB) are higher-power images of the boxed areas indicated in (I)–(L) and (U)–(X), respectively. Arrows indicate double-positive cells, arrowheads NFIA single-positive cells.

(CC) The percentage of Reelin$^+$ NFIA$^+$ cells is significantly different between the electroporated (E) sides of Pax6 and GFP embryos (***, $p < .001$), as well as between the E and contralateral (C) sides of Pax6 embryos (*, $p = .02$). The reduction in Slit1 expression on the E side of Pax6 embryos is significant with respect to both the C side (**, $p = .002$), and the E side of GFP controls (*, $p = .009$). Mean ± SEM; n = 5 embryos per condition; two independent experiments.

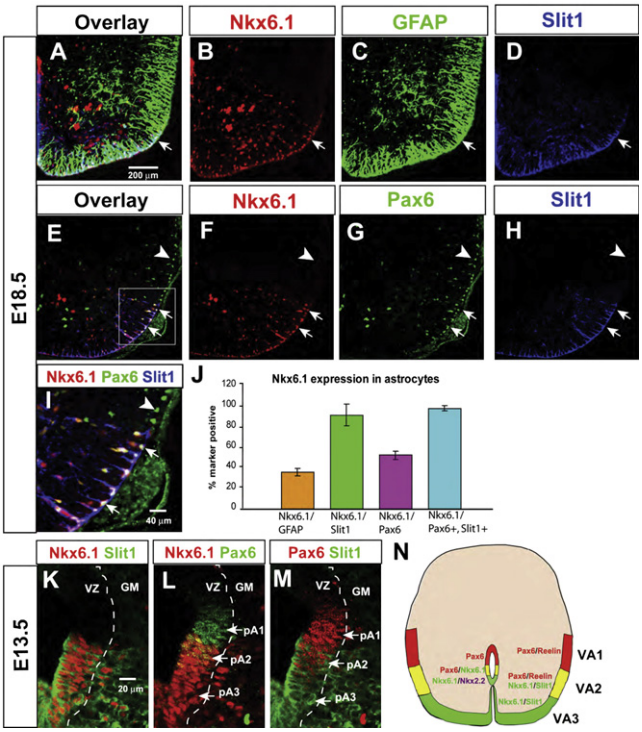

Figure 5. Nkx6.1 Is Coexpressed by Slit1$^+$ Astrocytes and Their Precursors

(A–I) Triple labeling for Nkx6.1, GFAP, and Slit1-GFP (A–D) or Nkx6.1, Pax6, and Slit1-GFP (E–I). (I) is a higher-power image of the boxed area in (E). Note that all Slit1$^+$ cells in this domain (boxed area, E) are Nkx6.1$^+$ and Pax6$^+$ (E–G, I; arrows, white nuclei), while all Pax6$^+$ cells dorsal to the boundary of Slit1 expression are Nkx6.1$^-$ (E–G, I; arrowheads).

(J) Quantification of Nkx6.1 expression in astrocyte subpopulations. Nkx6.1 is expressed in >90% of Slit1$^+$ astrocytes (green bar). Error bars represent mean ± SEM.

(K–M) Triple antibody labeling for Nkx6.1, Slit1-GFP, and Pax6 in the E13.5 VZ, displayed as pairwise comparisons from the same section. The three progenitor domains are indicated (L and M; arrows). "GM," gray matter.

(N) Composite schematic illustrating relationship between the domains of Reelin and Slit1 expression, and those of Pax6 and Nkx6.1 expression, in the white matter at E18.5 and in the VZ at E13.5.

pA2) also overlaps that of Nkx6.1 (Figure 5L, pA2). Taken together, these data suggest that Nkx6.1 is expressed by the VA3 (Pax6$^-$) and VA2 (Pax6$^+$) astrocyte subpopulations, and by their presumptive precursors (pA3 and pA2, respectively) but not by the VA1 astrocytes (Figure 5N).

Misexpression of Nkx6.1 Promotes Expression of Slit1 in WMAs

We wished to examine whether the expression of Nkx6.1 in Slit1$^+$ astrocytes reflects a functional role for this HD protein in the specification of astrocyte identity. As an initial step, we tested the prediction that misexpression of Nkx6.1 would promote an upregulation of Slit1 in dorso-lateral (VA1) astrocytes. Indeed, electroporation of Nkx6.1 in chick embryos using an RCAS (B) retroviral construct resulted in a clear induction of *Slit1* expression in the white matter on the electroporated side (Figures 6G and 6H versus 6I and 6J, WM; Figure 6QQ, Slit1). Colabeling for NFIA confirmed that this upregulation occurred in astrocytes (Figures 6P and 6V, arrow). Expression of Reelin was unaffected by misexpression of Nkx6.1 (Figures 6Y, 6BB, and 6QQ; Reelin). Induction of Slit1 was particularly evident in more dorso-lateral regions of the spinal cord, where Slit1$^-$ VA1 astrocytes are normally located (Figures 6I, 6J, 6O, 6P, 6U, and 6V, arrow). This phenotypic effect of Nkx6.1 misexpression was observed not only at brachial but also at lumbar axial levels (Figure S7), a location where such manipulations have no effect on the differentiation of V0–V2 interneurons (Briscoe et al., 2000). Nkx6.1 misexpression also promoted a dorsal expansion of Slit1 expression within the VZ at E5 (data not shown). Thus, this HD factor can positively regulate the positional boundaries of Slit1 expression, both in differentiated WMAs and also in astrocytic precursors within the germinal layer of the spinal cord.

The observation that Nkx6.1 positively regulates Slit1 expression, taken together with the fact that VA2 astrocytes coexpress both Nkx6.1 and Pax6, suggested that the reason Pax6 does not repress Slit1 in VA2, as it does in VA1, astrocytes is because Nkx6.1 overrides its repressive activity toward Slit1. To test this hypothesis, we asked whether coelectroporation of both Nkx6.1 and Pax6 would block the latter factor's ability to repress Slit1 expression in WMAs. In embryos misexpressing both Pax6 and Nkx6.1, not only did Pax6 fail to repress Slit1, but it also did not diminish the effect of Nkx6.1 to upregulate Slit1 expression (Figure 6H versus 6L, WM; Figure 6RR, Slit1). Interestingly, while Nkx6.1 overrode the ability of Pax6 to repress Slit1, it did not interfere with the activity of Pax6 to upregulate Reelin expression (Figure 6Z versus 6DD WM; Figure 6RR, Reelin).

Finally, we investigated whether the repression of Slit1 by Pax6 in VA1 astrocytes was mediated via repression of Nkx6.1. Examination of *Pax6$^{lacZ/lacZ}$; Slit1$^{eGFP/+}$* embryos indicated that the dorsal derepression of Slit1-GFP (Figure 3) was not accompanied by a derepression of Nkx6.1 (Figures S8B and S8E, arrows; Figure S8G). Thus, the derepression of Slit1 in VA1 astrocytes caused by mutation of Pax6 is Nkx6.1 independent. Examination of Nkx6.2, a related HD protein (Vallstedt et al., 2001), indicated that it is not expressed in the VZ or in WMAs at these gliogenic stages, in either wild-type or *Pax6* mutant embryos (Figures S5I–S5L) (data not shown). These data suggest that the Pax6-dependent repression of Slit1 in wild-type VA1 astrocytes is not mediated via repression of Nkx6.1, but by another mechanism.

DISCUSSION

We have demonstrated that the ventral spinal cord white matter contains at least three positionally distinct astrocyte subtypes in vivo, which can be identified by the combinatorial expression of the guidance molecules Reelin and Slit1. These distinct positional identities are specified by the HD transcription factors Pax6 and Nkx6.1, in a combinatorial manner. Thus, positional identity is an organizing feature of WMA diversity and is specified by a HD code, whose elements are reutilized following their role in the specification of neuronal identity (Figure 7A).

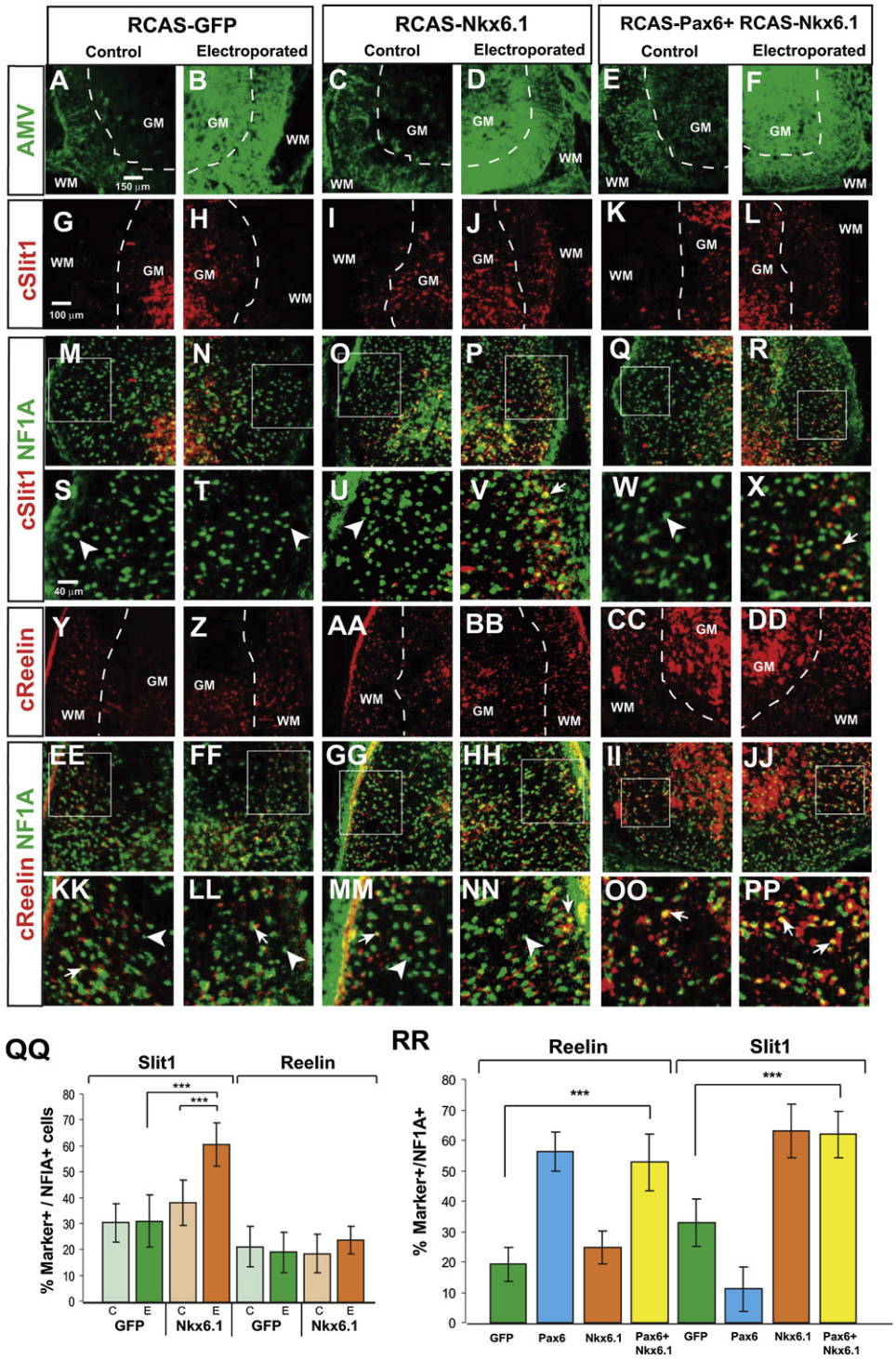

Figure 6. Nkx6.1 Promotes Slit1 Expression in Astrocytes and Overrides Its Repression by Pax6

(A–PP) Sections through the spinal cord of E12 chick embryos electroporated with the constructs indicated above the diagram and labeled with the antibodies (AMV, NF1A) or cRNA probes (cSlit1, cReelin) indicated to the left. Abbreviations are as in Figure 4. (M)–(R) and (EE)–(JJ) are the same panels as in (G)–(L) and (Y)–(DD), respectively, but include NFIA expression. (S)–(X) and (KK)–(PP) are higher-power images of the boxed areas indicated in (M)–(R) and (EE)–(JJ), respectively. Arrows in (S)–(X) and (KK)–(PP) indicate double-positive cells, arrowheads indicate NFIA single-positive cells.

(QQ) The percentage of Slit1+NFIA+ cells is significantly increased on the electroporated, or E, side of Nkx6.1 embryos, relative to either the control (C) side of the same embryos (***, p = .0003), or to the E side of GFP embryos (***, p < .001). n = 4 embryos per condition; two independent experiments.

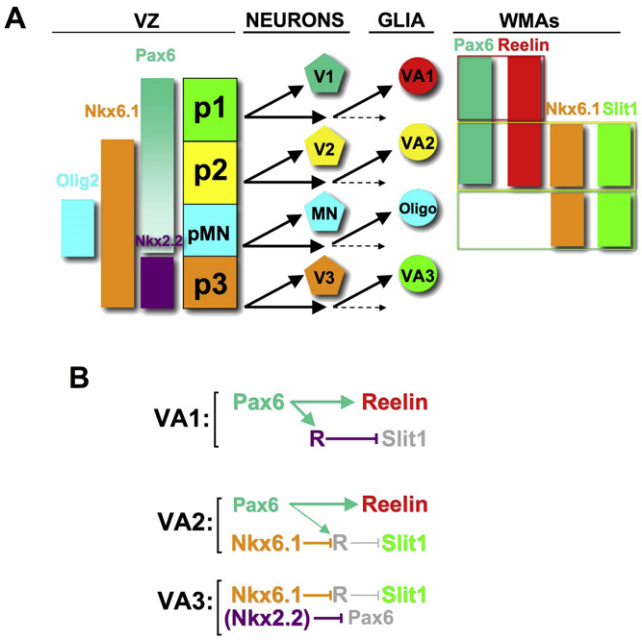

Figure 7. A Transcriptional Code for Astrocyte Positional Identity

(A) Schematic illustrating sequential generation of neurons and glia from different progenitor domains in the ventral spinal cord. VZ, ventricular zone; WMAs white matter astrocytes. The molecular phenotype of each of the three WMA subtypes is enclosed in a colored box. The three classes of WMAs are present in roughly equal proportions. Note that the expression boundaries of some of the transcription factors in the VZ shift from the neurogenic to the gliogenic phases; these shifts are omitted for simplicity. Note also that Nkx2.2, which is coexpressed with Nkx6.1 in the ventral-most (pA3) domain of the VZ during the gliogenic phase (Figure S6) is not coexpressed with Nkx6.1 in VA3 WMAs (Figure S7).

(B) Model for the regulation of astrocyte identity by Pax6 and Nkx6.1. R represents a hypothetical repressor of Slit1, which is activated by Pax6 and repressed by Nkx6.1. See Discussion for details. Repression of Pax6 by Nkx2.2 is likely important for the initial specification of VA3 identity within the VZ (see A), but does not contribute to the maintenance of VA3 identity in the WM.

Astrocytes in the Spinal Cord White Matter Exhibit Distinct Positional Identities

The recognition that positional differences underlie neuronal subtype diversity has aided both the identification and functional characterization of different neuronal subpopulations, as well as analysis of the developmental mechanisms that control their generation (Jessell, 2000; Briscoe and Ericson, 2001; Shirasaki and Pfaff, 2002). Here we provide evidence for molecular differences in the positional identities of WMA subpopulations within a specific region of the CNS. Previous studies have reported differences in the expression of markers such as ephrin-B1 and BLBP, by radial glial precursor cells at different locations along the dorsoventral axis of the VZ (Ogawa et al., 2005). However, these differences are not maintained by differentiated WMAs. The transcription factor SCL was shown to control generic aspects of astrocyte differentiation, in a position-specific manner (Muroyama et al., 2005), but no evidence was provided for any role in controlling position-specific phenotypic properties of WMAs.

The functional significance of the VA1–VA3 astrocyte subpopulations revealed by our studies is not yet clear. Reelin and Slit1 are secreted molecules involved in cell migration (Rice and Curran, 2001) and axon guidance (Brose et al., 1999; Plump et al., 2002), respectively. Slits in particular are expressed by astrocytic glia in the floorplate, a midline structure (Holmes et al., 1998; Brose et al., 1999; reviewed in Lemke, 2001). The combinatorial expression of these molecules by subsets of WMAs therefore suggests a potential role for this heterogeneity in guiding axonal trajectory and/or cell migration (Powell et al., 1997). Interestingly, Reelin is expressed not only by VA1 and VA2 astrocytes, but also by V1 and V2 interneurons (Yip et al., 2004b). The dorsal restriction of Reelin expression is thought to be important in guiding the migration of sympathetic preganglionic motoneurons, within the spinal cord (Yip et al., 2004b, 2007). Perhaps the expression of Reelin by VA1 and VA2 astrocytes contributes to this guidance process. In addition to their role in axon guidance, astrocytes are important for enhancing synapse formation and synaptic efficacy (Pfrieger and Barres, 1997; Ullian et al., 2001, 2004). Perhaps astrocytes derived from a particular progenitor domain preferentially enhance synapse formation by neuronal subtypes derived from the same progenitor domain.

A Transcriptional Code for Astrocyte Positional Identity

Our data support a combinatorial model for the specification of astrocyte positional identity, in which expression of Pax6 in the absence of Nkx6.1 specifies a VA1 phenotype (Reelin$^+$, Slit1$^-$), coexpression of Pax6 and Nkx6.1 specifies a VA2 phenotype (Reelin$^+$, Slit1$^+$), and expression of Nkx6.1 in the absence of Pax6 specifies a VA3 phenotype (Slit1$^+$, Reelin$^-$) (Figure 7A). Nkx2.2 may also participate in this code by repressing Reelin in pA3 VZ precursors (Figure S5) via repression of Pax6 (Briscoe et al., 1999), an activity that Nkx6.1 lacks (Briscoe et al., 2000). Consistent with this, misexpression of Nkx2.2 strongly repressed Reelin and upregulated Slit1 in the VZ at E5 (data not shown). However Nkx2.2, unlike Nkx6.1, is not expressed in differentiated Slit1$^+$ WMAs (Figure S6), but rather in oligodendrocytes (Qi et al., 2001; Zhou et al., 2001). Therefore, the maintenance of Slit1 expression in VA3 WMAs is more likely to involve Nkx6.1.

Our data suggest that the coexpression of Slit1 and Reelin in VA2 astrocytes reflects a role for Nkx6.1 to override repression of *Slit1* by Pax6, without interfering with its activation of Reelin. Consistent with this view, Nkx6.1 is able to prevent repression of Slit1 by Pax6 in coelectroporation experiments, while permitting Pax6 enhancement of Reelin expression (Figure 6RR). Since Nkx6.1 can act either as an activator or as a repressor, depending on context (Taylor et al., 2005), it could either directly activate *Slit1* transcription in VA2 precursors, or do so indirectly, by

(RR) Bars represent mean ± SEM from the E side only. The data from embryos electroporated with Pax6 alone (blue bars) or Nkx6.1 alone (orange bars) are reproduced from Figures 4CC and 6QQ, respectively, and included for comparative purposes. The percentage of Slit1+NFIA+ cells in embryos misexpressing both Nkx6.1 and Pax6 is significantly higher than in GFP controls (Slit1, ***, $p < .001$) and is similar to that in embryos expressing Nkx6.1 alone (QQ). n = 4 embryos per condition, two independent experiments.

repressing an as-yet-unidentified repressor (Figure 7B). The latter model seems more likely, because in *Pax6* mutants, Slit1 is derepressed in Pax6-lacZ$^+$ VA1 astrocytes without derepression of Nkx6.1 (Figure S9). Thus, Nkx6.1 is not essential for Slit1 derepression in the absence of Pax6 function. This in turn suggests that, in wild-type embryos, the absence of Slit1 in VA1 astrocytes reflects either direct repression of *Slit1* by Pax6, or else a Pax6-dependent *Slit1* repressor. We favor the latter explanation, because in the former case, one might expect that Slit1 expression would only occur in ventral astrocytes lacking Pax6, and this is not observed (Figures 5I and 5J). We suggest that in VA2 astrocytes, Nkx6.1 may repress a Pax6-dependent repressor of Slit1 (Figure 7B, VA2). A similar layered-repression model has been proposed to explain the role of Nkx6.1 in controlling IN identity (Vallstedt et al., 2001). Interestingly, it has recently been shown that Nkx6.1 dominantly antagonizes the activation of glucagon transcription by Pax6 in pancreatic α cells, via competition for binding to common promoter elements (Gauthier et al., 2007). A similar antagonism may allow coexpression of Pax6 and Slit1 in VA2 astrocytes expressing Nkx6.1.

Timing and Location of HD Influences on Astrocyte Positional Identity

The genetic evidence supporting a role for Pax6 and Nkx6.1 in specifying astrocyte identity leaves open the question of when and where these HD factors act. Several lines of evidence suggest that astrocyte positional identity is initially specified within the VZ. First, Pax6 and Reelin are coexpressed within the VZ in NFIA$^+$ glial progenitor cells, as are Nkx6.1 and Slit1. With the exception of the Olig2$^+$ domain, therefore, there is continuity in the coexpression of these HD and guidance molecules from the germinal layer to the white matter, an interpretation supported by BrdU pulse-chase experiments (Figure S2). Second, in embryos electroporated with Pax6 at E2, ventral expansion of Reelin expression is detected in NF1A$^+$ glial progenitors in the VZ at E5-E6 (Figure S4). Importantly, a similar result is obtained when electroporation is performed at E4.5 (Figure S4), by which stage ventral neurogenesis has ended (Deneen et al., 2006). This latter result argues that the effect of Pax6 on Reelin is unlikely to be due to indirect effects on neuronal identity specification at earlier stages. In support of this conclusion, loss- and gain-of-function manipulations of these HD factors cause changes in astrocytic expression of Reelin and Slit1 at positions along the rostrocaudal axis where similar manipulations do not cause changes in the number or distribution of ventral IN subtypes (data not shown) (Burrill et al., 1997; Ericson et al., 1997; Osumi et al., 1997; Takahashi and Osumi, 2002; Novitch et al., 2003). Taken together, these data support the idea that astrocyte positional identity is specified within the germinal layer, prior to emigration of astrocyte precursors into the gray matter. Importantly, however, the continued expression of Pax6 and Nkx6.1 in WMAs raises the possibility that these proteins play a role in the maintenance of astrocyte positional identity as well as in its initial specification (Figure 7A).

The data presented here provide evidence that positional identity is an organizing principle underlying phenotypic diversity among WMAs, as well as among neurons. They also suggest that positional mechanisms are involved in the developmental specification of this heterogeneity within the VZ. Our results argue against the view that astrocyte heterogeneity in the CNS primarily reflects the phenotypic plasticity of such glia, in response to local environmental signals, after they migrate and differentiate. Instead, the data suggest that at least some aspects of astrocyte diversity are prespecified within the germinal zone of the CNS, by mechanisms that are not only analogous to those that specify neuronal identity at earlier stages, but which employ elements of the same transcriptional code. From this perspective, elements of this code can be thought of as coupling the specification of positionally distinct neuronal subtypes, to positionally distinct glial subtypes, a generalization of a concept first established for *Olig2* and its role in specifying motoneuron and oligodendrocyte fate (Lu et al., 2002; Zhou and Anderson, 2002; Muroyama et al., 2005). Our findings open up for future study the function of the astrocyte subtypes we have identified in the spinal cord, as well as the extent to which positional specification mechanisms generate astrocyte diversity in other regions of the CNS.

EXPERIMENTAL PROCEDURES

Mouse Mutants

Olig1,2$^{-/-}$ mice (Zhou and Anderson, 2002), *Pax6-lacZ* mice (St-Onge et al., 1997), and *Slit1-GFP mice* (Plump et al., 2002) were genotyped by PCR using *lacZ* and *GFP* primers. *Pax6-lacZ* mice were intercrossed with *Slit1-GFP* mice to generate *Pax6*$^{-/-}$, *Slit1-GFP*$^{+/-}$, and *Pax6*$^{+/-}$, *Slit1-GFP*$^{+/-}$ embryos for analysis.

FACS and Microarray Experiments

Olig2-GFP-expressing cells were FACS isolated from spinal cords of *Olig1,2*$^{+/-}$ and *Olig1,2*$^{-/-}$ embryos as previously described (Mukouyama et al., 2006). RNA was extracted from the isolated cells, amplified, biotinylated, and hybridized to Affymetrix mU74v2 A, B, and C chips (Deneen et al., 2006). Analysis of microarray data was performed using Affymetrix Microarray Suite and Rosetta Resolver software.

In Situ Hybridization

Nonradioactive in situ hybridization using DIG-labeled (Zhou et al., 2000) or fluorescent probes (Choi et al., 2005) was performed on frozen sections of mouse or chick spinal cord as described. The following probes were used: mouse Reelin (gift of Gabriella D'Arcangelo), mouse Slit1 (gift of Marc Tessier-Lavigne), chick Reelin, and chick Slit1 (gift of Ed Laufer). Antibodies used are listed in Supplemental Data.

Chick Embryo Electroporation

Chick embryos were electroporated at E2 with either RCAS(B) GFP, RCAS(B) Pax6, or RCAS(B) Nkx6.1 replication-competent avian retroviruses using established methods (Zhou et al., 2001). The electroporation conditions were 5 square wave pulses of 50 ms duration at 24 V. Embryos were incubated in a humidified 37°C incubator until E12.

SUPPLEMENTAL DATA

Supplemental Data include nine figures and can be found with this article online at http://www.cell.com/cgi/content/full/133/3/510/DC1/.

ACKNOWLEDGMENTS

We thank A. Stoykova, P. Gruss, and G. Lanuza for sharing Pax6-lacZ mice and embryos, M. Tessier-Lavigne for the Slit1-GFP mice, and K. McCarthy for pilot experiments with GFAP-CreER mice. We also thank T. Jessell for helpful discussions and antibodies, and E. Laufer and G. D'Arcangelo for in situ probes and antibody reagents. We thank S. Pease, J. Alex, and the staff of

the Caltech animal facility for assistance with mouse breeding and timed matings; R. Diamond for assistance with FACS; E. Zuo for Affymetrix microarray hybridization; P. Lwigale for advice and assistance with electroporation and egg husbandry techniques; M. Martinez for genotyping mouse lines; J. Chow, M. Lee, R. Ho, and J. S. Chang for technical assistance; G. Mosconi for laboratory management; and G. Mancuso for administrative assistance. This work was supported in part by NIH grant 1RO1-NS23476. D.J.A. is an Investigator of the Howard Hughes Medical Institute.

Received: September 9, 2007
Revised: December 20, 2007
Accepted: February 11, 2008
Published: May 1, 2008

REFERENCES

Bailey, M.S., and Shipley, M.T. (1993). Astrocyte subtypes in the rat olfactory bulb: Morphological heterogeneity and differential laminar distribution. J. Comp. Neurol. *328*, 501–526.

Briscoe, J., and Ericson, J. (2001). Specification of neuronal fates in the ventral neural tube. Curr. Opin. Neurobiol. *11*, 43–49.

Briscoe, J., Sussel, L., Serup, P., Hartigan-O'Connor, D., Jessell, T.M., Rubenstein, J.L., and Ericson, J. (1999). Homeobox gene Nkx2.2 and specification of neuronal identity by graded Sonic hedgehog signalling. Nature *398*, 622–627.

Briscoe, J., Pierani, A., Jessell, T.M., and Ericson, J. (2000). A homeodomain protein code specifies Progenitor cell identity and neuronal fate in the ventral neural tube. Cell *101*, 435–445.

Brose, K., Bland, K.S., Wang, K.H., Arnott, D., Henzel, W., Goodman, C.S., Tessier-Lavigne, M., and Kidd, T. (1999). Slit proteins bind Robo receptors and have an evolutionarily conserved role in repulsive axon guidance. Cell *96*, 795–806.

Burrill, J.D., Moran, L., Goulding, M.D., and Saueressig, H. (1997). PAX2 is expressed in multiple spinal cord interneurons, including a population of EN1+ interneurons that require PAX6 for their development. Development *124*, 4493–4503.

Choi, G.B., Dong, H.-w., Murphy, A.J., Valenzuela, D.M., Yancopoulos, G.D., Swanson, L.W., and Anderson, D.J. (2005). Lhx6 delineates a pathway mediating innate reproductive behaviors from the amygdala to the hypothalamus. Neuron *46*, 647–660.

D'Ambrosio, R., Wenzel, J., Schwartzkroin, P.A., McKhann, G.M., II, and Janigro, D. (1998). Functional specialization and topographic segregation of hippocampal astrocytes. J. Neurosci. *18*, 4425–4438.

Deneen, B., Ho, R., Lukaszewicz, A., Hochstim, C.J., Gronostajski, R.M., and Anderson, D.J. (2006). The transcription factor NFIA controls the onset of gliogenesis in the developing spinal cord. Neuron *52*, 953–968.

Ericson, J., Rashbass, P., Schedl, A., Brenner-Morton, S., Kawakami, A., van Heyningen, V., Jessell, T.M., and Briscoe, J. (1997). Pax6 controls progenitor cell identity and neuronal fate in response to graded Shh signaling. Cell *90*, 169–180.

Fields, R.D., and Stevens-Graham, B. (2002). New insights into neuron-glia communication. Science *298*, 556–562.

Fu, H., Qi, Y., Tan, M., Cai, J., Hu, X., Liu, Z., Jensen, J., and Qiu, M. (2003). Molecular mapping of the origin of postnatal spinal cord ependymal cells: evidence that adult ependymal cells are derived from Nkx6.1+ ventral neural progenitor cells. J. Comp. Neurol. *456*, 237–244.

Gabay, L., Lowell, S., Rubin, L.L., and Anderson, D.J. (2003). Deregulation of dorsoventral patterning by FGF confers trilineage differentiation capacity on CNS stem cells in vitro. Neuron *40*, 485–499.

Gauthier, B.R., Gosmain, Y., Mamin, A., and Philippe, J. (2007). The β-cell specific transcription factor Nkx6.1 inhibits glucagon gene transcription by interfering with Pax6. Biochem. J. *403*, 593–601.

Goulding, M., and Lamar, E. (2000). Neuronal patterning: Making stripes in the spinal cord. Curr. Biol. *10*, R565–R568.

Holmes, G.P., Negus, K., Burridge, L., Raman, S., Algar, E., Yamada, T., and Little, M.H. (1998). Distinct but overlapping expression patterns of two vertebrate slit homologs implies functional roles in CNS development and organogenesis. Mech. Dev. *79*, 57–72.

Jessell, T.M. (2000). Neuronal Specification in the spinal cord: inductive signals and transcriptional codes. Nat. Rev. Genet. *1*, 20–29.

Kubasak, M.D., Brooks, R., Chen, S., Villeda, S.A., and Phelps, P.E. (2004). Developmental distribution of reelin-positive cells and their secreted product in the rodent spinal cord. J. Comp. Neurol. *468*, 165–178.

Lemke, G. (2001). Glial control of neuronal development. Annu. Rev. Neurosci. *24*, 87–105.

Liuzzi, F.J., and Miller, R.H. (1987). Radially oriented astrocytes in the normal adult rat spinal cord. Brain Res. *403*, 385–388.

Lu, Q.R., Sun, T., Zhu, Z., Ma, N., Garcia, M., Stiles, C.D., and Rowitch, D.H. (2002). Common developmental requirement for Olig function indicates a motor neuron/oligodendrocyte connection. Cell *109*, 75–86.

McMahon, A.P. (2000). Neural patterning: The role of Nkx genes in the ventral spinal cord. Genes Dev. *14*, 2261–2264.

Miller, R.H., and Raff, M.C. (1984). Fibrous and protoplasmic astrocytes are biochemically and developmentally distinct. J. Neurosci. *4*, 585–592.

Miller, R.H., Zhang, H., and Fok-Seang, J. (1994). Glial cell heterogeneity in the mammalian spinal cord. Perspect. Dev. Neurobiol. *2*, 225–231.

Mori, S., and Leblond, C.P. (1969). Electron microscopic features and proliferation of astrocytes in the corpus callosum of the rat. J. Comp. Neurol. *137*, 197–225.

Mukouyama, Y.S., Deneen, B., Lukaszewicz, A., Novitch, B.G., Wichterle, H., Jessell, T.M., and Anderson, D.J. (2006). Olig2+ neuroepithelial motoneuron progenitors are not multipotent stem cells in vivo. Proc. Natl. Acad. Sci. USA *103*, 1551–1556.

Muroyama, Y., Fujiwara, Y., Orkin, S.H., and Rowitch, D.H. (2005). Specification of astrocytes by bHLH protein SCL in a restricted region of the neural tube. Nature *438*, 360–363.

Novitch, B.G., Wichterle, H., Jessell, T.M., and Sockanathan, S. (2003). A requirement for retinoic acid-mediated transcriptional activation in ventral neural patterning and motor neuron specification. Neuron *40*, 81–95.

Ogawa, Y., Takebayashi, H., Takahashi, M., Osumi, N., Iwasaki, Y., and Ikenaka, K. (2005). Gliogenic radial glial cells show heterogeneity in the developing mouse spinal cord. Dev. Neurosci. *27*, 364–377.

Osumi, N., Hirota, A., Ohuchi, H., Nakafuku, M., Iimura, T., Kuratani, S., Fujiwara, M., Noji, S., and Eto, K. (1997). Pax-6 is involved in the specification of hindbrain motor neuron subtype. Development *124*, 2961–2972.

Pfrieger, F.W., and Barres, B.A. (1997). Synaptic efficacy enhanced by glial cells in vitro. Science *277*, 1684–1687.

Plump, A.S., Erskine, L., Sabatier, C., Brose, K., Epstein, C.J., Goodman, C.S., Mason, C.A., and Tessier-Lavigne, M. (2002). Slit1 and Slit2 cooperate to prevent premature midline crossing of retinal axons in the mouse visual system. Neuron *33*, 219–232.

Powell, E.M., Meiners, S., DiProspero, N.A., and Geller, H.M. (1997). Mechanisms of astrocyte-directed neurite guidance. Cell Tissue Res. *290*, 385–393.

Pringle, N.P., Yu, W.-P., Howell, M., Colvin, J.S., Ornitz, D.M., and Richardson, W.D. (2003). Fgfr3 expression by astrocytes and their precursors: evidence that astrocytes and oligodendrocytes originate in distinct neuroepithelial domains. Development *130*, 93–102.

Qi, Y., Cai, J., Wu, Y., Wu, R., Lee, J., Fu, H., Rao, M., Sussel, L., Rubenstein, J., and Qiu, M. (2001). Control of oligodendrocyte differentiation by the Nkx2.2 homeodomain transcription factor. Development *28*, 2723–2733.

Raff, M.C. (1989). Glial cell diversification in the rat optic nerve. Science *243*, 1450–1455.

Raff, M.C., Abney, E.R., and Miller, R.H. (1984). Two glial cell lineages diverge prenatally in rat optic nerve. Dev. Biol. *106*, 53–60.

Rice, D.S., and Curran, T. (2001). Role of the reelin signaling pathway in central nervous system development. Annu. Rev. Neurosci. *24*, 1005–1039.

Sharif, A., Renault, F., Beuvon, F., Castellanos, R., Canton, B., Barbeito, L., Junier, M.P., and Chneiweiss, H. (2004). The expression of PEA-15 (phosphoprotein enriched in astrocytes of 15 kDa) defines subpopulations of astrocytes and neurons throughout the adult mouse brain. Neuroscience *126*, 263–275.

Shibata, T., Yamada, K., Watanabe, M., Ikenaka, K., Wada, K., Tanaka, K., and Inoue, Y. (1997). Glutamate transporter GLAST is expressed in the radial glia-astrocyte lineage of developing mouse spinal cord. J. Neurosci. *17*, 9212–9219.

Shirasaki, R., and Pfaff, S.L. (2002). Transcriptional codes and the control of neuronal identity. Annu. Rev. Neurosci. *25*, 251–281.

St-Onge, L., Sosa-Pineda, B., Chowdhury, K., Mansouri, A., and Gruss, P. (1997). Pax6 is required for differentiation of glucagon-producing [alpha]-cells in mouse pancreas. Nature *387*, 406–409.

Sugimori, M., Nagao, M., Bertrand, N., Parras, C.M., Guillemot, F., and Nakafuku, M. (2007). Combinatorial actions of patterning and HLH transcription factors in the spatiotemporal control of neurogenesis and gliogenesis in the developing spinal cord. Development *134*, 1617–1629.

Takahashi, M., and Osumi, N. (2002). Pax6 regulates specification of ventral neurone subtypes in the hindbrain by establishing progenitor domains. Development *129*, 1327–1338.

Taylor, D.G., Babu, D., and Mirmira, R.G. (2005). The C-terminal domain of the beta cell homeodomain factor Nkx6.1 enhances sequence-selective DNA binding at the insulin promoter. Biochemistry *44*, 11269–11278.

Ullian, E.M., Christopherson, K.S., and Barres, B.A. (2004). Role for glia in synaptogenesis. Glia *47*, 209–216.

Ullian, E.M., Sapperstein, S.K., Christopherson, K.S., and Barres, B.A. (2001). Control of synapse number by glia. Science *291*, 657–661.

Vallstedt, A., Muhr, J., Pattyn, A., Pierani, A., Mendelsohn, M., Sander, M., Jessell, T.M., and Ericson, J. (2001). Different levels of repressor activity assign redundant and specific roles to Nkx6 genes in motor neuron and interneuron specification. Neuron *31*, 743–755.

Vaughn, J.E., and Pease, D.C. (1967). Electron microscopy of classically stained astrocytes. J. Comp. Neurol. *131*, 143–154.

Yip, Y.P., Capriotti, C., Magdaleno, S., Benhayon, D., Curran, T., Nakajima, K., and Yip, J.W. (2004a). Components of the reelin signaling pathway are expressed in the spinal cord. J. Comp. Neurol. *470*, 210–219.

Yip, Y.P., Zhou, G., Capriotti, C., and Yip, J.W. (2004b). Location of preganglionic neurons is independent of birthdate but is correlated to reelin-producing cells in the spinal cord. J. Comp. Neurol. *475*, 564–574.

Yip, Y.P., Kronstadt-O'Brien, P., Capriotti, C., Cooper, J.A., and Yip, J.W. (2007). Migration of sympathetic preganglionic neurons in the spinal cord is regulated by Reelin-dependent Dab1 tyrosine phosphorylation and CrkL. J. Comp. Neurol. *502*, 635–643.

Zhou, Q., and Anderson, D.J. (2002). The bHLH transcription factors OLIG2 and OLIG1 couple neuronal and glial subtype specification. Cell *109*, 61–73.

Zhou, Q., Wang, S., and Anderson, D.J. (2000). Identification of a novel family of oligodendrocyte lineage-specific basic helix-loop-helix transcription cactors. Neuron *25*, 331–343.

Zhou, Q., Choi, G., and Anderson, D.J. (2001). The bHLH transcription factor Olig2 promotes oligodendrocyte differentiation in collaboration with Nkx2.2. Neuron *31*, 791–807.